Mean Fluxes of Visible Solar Radiation in Broken Clouds

V. E. Zuev, G. A. Titov, T. B. Zhuravleva, and S. Y. Popov
Institute of Atmospheric Optics, Siberian Branch
Russian Academy of Sciences
Tomsk, Russia

Introduction

Generally, radiation codes for general circulation models (GCMs) include, together with other procedures, calculations of vertical profiles of upward and downward radiation fluxes which are needed to calculate radiant heat influxes. These last radiative characteristics serve as an input for a number of atmospheric processes predicted from GCMs, e.g., the equation of radiant heat influxes is sometimes a starting point for modeling the formation and evolution of cloud fields; the equation of heat balance of the earth's surface involves solar and thermal radiation fluxes that govern the surface thermal regime; and so forth. Because calculation errors can significantly affect the description of these processes, of importance is the question of the accuracy of determinations of the upward and downward radiation fluxes at different atmospheric levels.

Most of the present GCM codes make use of the models of plane-parallel, horizontally homogeneous atmosphere and are based computationally on solving the equation of radiative transfer using deterministic optical characteristics. In the presence of clouds partially covering the sky, flux values represent a linear combination of clear- and overcast-sky fluxes weighted by a specific value of cloud fraction. Such an approach is adequate for the stratus-clouds-only cases, when the parameter $\gamma \approx 0$ (with $\gamma = H/D$, H the cloud layer thickness, and D the mean horizontal cloud size). Under the cumulus cloud conditions ($\gamma \approx 1$), the approach can be regarded merely as a first, fairly crude approximation (Skorinov and Titov 1984; Titov 1987), recognizing that the shortwave radiative transfer is affected remarkably by the stochastic geometry of cloud fields.

Mean albedo and transmission of shortwave radiation in the system "clouds-aerosol-underlying surface" are sufficiently investigated (Titov 1989; Zhuravleva 1993; Zuev and Titov 1994). In the present work, we raise the question about the value of the effect the cloud field random geometry has on the mean upward and downward fluxes of the visible and near-IR solar radiation throughout the atmosphere. To this end, computations of the vertical profiles of radiant fluxes in cumulus are compared with those in equivalent (i.e., with the same optical characteristics) stratus. Treatment across the visible spectrum can be restricted to a discussion of results for a single wavelength, as the cloud optical characteristics change slightly, while the gaseous absorption is absent in this spectral range. In the near-IR spectral range, mean fluxes are computed at once for a certain subinterval $\Delta\nu$ whose width is determined by the spectral resolution of exploited transmission functions of atmospheric gases (for our case, $\Delta\nu \approx 10 \div 20\ cm^{-1}$).

Model of Atmosphere

Atmosphere is considered as a set of N_{lay} homogeneous layers, each characterized by atmospheric parameters assumed to be constant. Clouds are always separated as an individual layer with the lower, H^b_{cl}, and upper, H^t_{cl}, boundaries (Figure 1). When an atmosphere is divided, its layers should be chosen in accordance with those used in familiar GCMs. At present, there are quite a large number of GCM versions that differ, in particular, in their computational layering (e.g., see Ellingson et al. [1991] and Fouquart et al. [1991] and bibliography therein). For instance, the computation levels can be defined by isobaric surfaces of 1000, 850, 700, 500, 400, 300, 250, 200, 150, 100 hPa. Realizing that it is impossible to create a universal

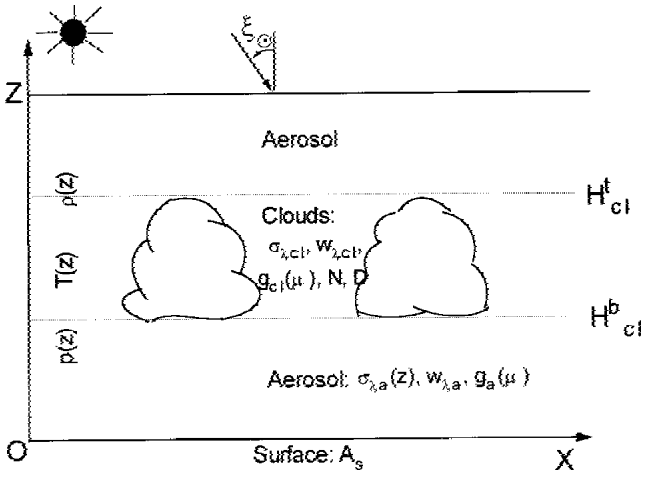

Figure 1. Model of atmosphere.

radiation code fitting all of the existing GCM versions, we chose to divide the atmosphere with the above indicated levels. Importantly, computations, if necessary, can be extended to involve any isobaric surfaces specified; the same is valid for the transmission functions of atmospheric gases we report below.

The vertical stratification and spectral behaviors of the aerosol extinction coefficient and the single scattering albedo are chosen to correspond to the mean-cyclic aerosol model (Zuev and Krekov 1986). To account for the absorption of solar radiation by water vapor and carbon dioxide, we use the model of transmission function (Golubitskii and Moskalenko 1968; Moskalenko 1969; Filippov 1973) defined as

$$P_{\Delta\nu} = \exp(-\beta_\nu (w^*)^{m_\nu})$$

with the spectral resolution $\Delta\nu \approx 10 \div 20\ cm^{-1}$. Here w^* is the equivalent (reduced) absorber mass which in a plane-stratified atmosphere in a layer $\{z_1, z_2\}$ is defined by the formula

$$w^* = \frac{1}{\cos\theta} \int_{z_1}^{z_2} \rho(z) \left(\frac{p(z)}{p_0} \right)^{n_\nu} dz$$

where

$\rho(z)$ and $p(z)$ are the absorber concentration and the pressure (in atm) at height z, respectively

$p_0 = 1$ atm is the pressure at $z = 0$

θ is the zenith viewing angle

In computations, we use the altitude profile of water vapor for the mid-latitude summer atmosphere (Zuev and Komarov 1986). Carbon dioxide is assumed to be uniformly mixed in altitude up to 100 hPa.

Clouds occupy the layer $1 \le z \le 1.5\ km$. A broken cloud model used as well as the Monte Carlo algorithm for calculating the mean fluxes of upward and downward solar radiation, both are given in detail in Titov et al.[(a)] The underlying surface reflects according to Lambert's law. Radiant fluxes are provided in relative units, the absolute values can be obtained by multiplying these by $\pi S_\lambda \cos\xi_\oplus$, with πS_λ the spectral solar constant, $\xi_\oplus$, the zenith solar angle.

Numerical Results

The above- and under-cloud atmospheres are optically thin compared with clouds. Thus, in the absence of gaseous absorption, vertical profiles of fluxes outside the clouds will be practically unchanged from the mean fluxes at the cloud layer boundaries. Therefore, of most interest in this spectral interval are vertical profiles of the mean fluxes within the cloudy layer, and we therefore confine ourselves to treating this atmospheric layer alone. Below, the results of computations at a wavelength $\lambda = 0.71\ \mu m$ are given, unless otherwise indicated.

We let $Q_{s,St}(z)$ and $Q_{s,Cu}(z)$ denote the mean downward fluxes, while $R_{St}(z)$ and $R_{Cu}(z)$ the mean upward fluxes of the scattered radiation, in stratus and cumulus clouds, respectively (brackets, meaning averages, are dropped for convenience).

(a) Titov, G. A., T. B. Zhuravleva, and V. E. Zuev. 1994. Mean radiant fluxes in the near-IR spectral range: algorithms for calculation. Submitted to *J. Geoph. Res.*

At $A_s = 0$, for upward fluxes the inequalities hold: $R_{Cu}(z) < R_{St}(z)$ for $\xi_\oplus = 0°$, and $R_{Cu}(z) > R_{St}(z)$ for $\xi_\oplus = 60°$ (Figure 2a). In a deterministic scattering medium, the flux of downward diffuse radiation has maximum for a certain optical depth. Analogous maximum is observed in the broken cloud case (Figure 2b). Differences between $Q_{s,St}(z)$ and $Q_{s,Cu}(z)$ are most dramatic at large $\xi_\oplus$ values. For $\xi_\oplus = 60°$, the maximum of $Q_{s,Cu}(z)$ sinks deeper from the upper cloud boundary and becomes flatter, as compared with the stratus cloud case. Differences in the mean fluxes of upward radiation between cumulus and equivalent stratus clouds are caused by the effects associated with the random geometry of cloud field and are discussed in detail in Titov (1987).

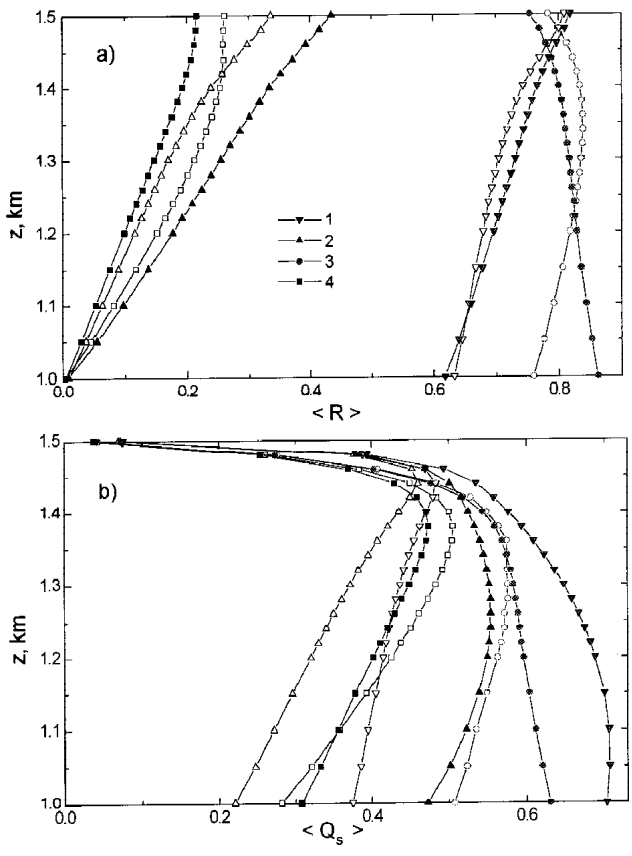

Figure 2. Mean fluxes of upward (a) and downward (b) radiation with $\sigma = 30\ km^{-1}$, $w_\lambda = 1$, $N = 0.5$, $D = 0.25\ km$ and for different solar zenith angles and surface albedos: (1,2) $\xi_\oplus = 0°$, (3,4) $\xi_\oplus = 60°$, (1,3) $A_s = 0$, (2,4) $A_s = 0.8$. Here and in Figures 3, 4, and 6, symbols are solid for cumulus and open for stratus.

Now we address the impact of reflection from the surface ($A_s > 0$) on the vertical profiles of the mean fluxes. Surface-reflected radiation can be viewed as a diffuse source illuminating the bottom of the atmosphere. Power and angle structure of radiation of this source depend upon the amount and angle structure of downward radiation at the surface level (plane $z = 0$), as well as upon the law of reflection from the surface. We let $R_d(z)$ and $Q_d(z)$ denote the mean upward and downward fluxes, provided that the bottom of the atmosphere is illuminated by an isotropic point source of unit power emitting into the upward hemisphere. Here and below, the index "*d*" stands for the corresponding fluxes calculated for the diffuse source. It is convenient to represent the solution of the problem in terms of the series in orders of reflection from the surface. We let $R^{(n)}(z)$ and $Q^{(n)}(z)$ denote contributions to the mean upward and downward fluxes by the nth reflection order, with $n = 1, 2,\ldots$. It is obvious that

$$R^{(1)}(z) = A_S[S(0) \quad \text{?}_S(0)]Q_d(z),\ Q^{(1)}(z) = A_S[S(0) \quad \text{?}_S(0)]R_d(z)$$

$$R^{(n)}(z) = A_S Q^{(n-1)}(0)Q_d(z),\ Q^{(n)}(z) = A_S Q^{(n-1)}(0)R_d(z),\ n = 2,$$

where $S(z)$ is the mean flux of direct radiation for $A_s = 0$; $Q_d(z) = S_d(z) + Q_{s,d}(z)$. The fluxes $S_d(z)$, $Q_{s,d}(z)$, and $R_d(z)$ can be obtained by integrating, with known weight function, the fluxes S, Q_s, and R over solar zenith angle. The mean-value theorem dictates that $S_d(z)$, $Q_{s,d}(z)$, and $R_d(z)$ will be proportional to S, Q_s, and R calculated for certain intermediate values of solar zenith angle and for $A_s = 0$. Therefore, it can be expected that the vertical profiles of $Q_{s,d}(z)$ and $R_d(z)$ will agree qualitatively with those of Q_s and R at $A_s = 0$. Obviously, $S_d(z)$ will be the decreasing function of z. Thus, for $A_s > 0$, a vertical profile of fluxes represents the sum of functions varying diversely and perhaps nonmonotonically with z. Hence, the profiles will depend upon which of the summands dominates at a given z. This explains why the flux profiles for $A_s > 0$ may qualitatively differ from the corresponding profiles for $A_s = 0$ (Figure 2).

Figure 2 illustrates flux computations in cumulus performed for $\gamma = 2$. This γ value is close to a maximum one ever observed. So, it is hoped that this figure gives the maximum

possible differences in radiation fluxes between cumulus and stratus clouds. Obviously, with decreasing γ, these differences will diminish.

As expected, maximum differences between upward and downward radiation fluxes occur for intermediate cloud fractions (Figure 3). At small *N*, downward radiation fluxes first rapidly grow in the upper portion of cloud layer and then change little, with decreasing altitude.

Dependence of the flux profiles upon cloud extinction coefficient is illustrated in Figure 4. Observe that a decrease in extinction coefficient is accompanied by a readily explainable shift of the maximum of the radiation flux downward into the cloud layer interior.

It is commonly assumed that clouds scatter conservatively in the visible spectral range (i.e., the single scattering albedo $w_\lambda = 1$). However, aerosol particles, such as soot, present as condensation nuclei can lower the w_λ value. Presence in broken clouds of even weak particulate absorption can significantly reduce (by tens of percents) the mean albedo and transmission (Titov 1987). Let us consider the vertical profiles of the mean absorption inside the cloud layer.

We divide the cloud layer into *M* sublayers with boundaries $z_i = const$, $i = 1,..., M, M + 1$, $z_1 = H^b_{cl}$, $z_{M+1} = H^t_{cl}$. Let $P(z_i,z_{i+1})$ denote the mean absorption in a sublayer (z_i,z_{i+1}). Then $P(z_l,z_{M+1})$ the mean absorption in the cloud layer, is defined as

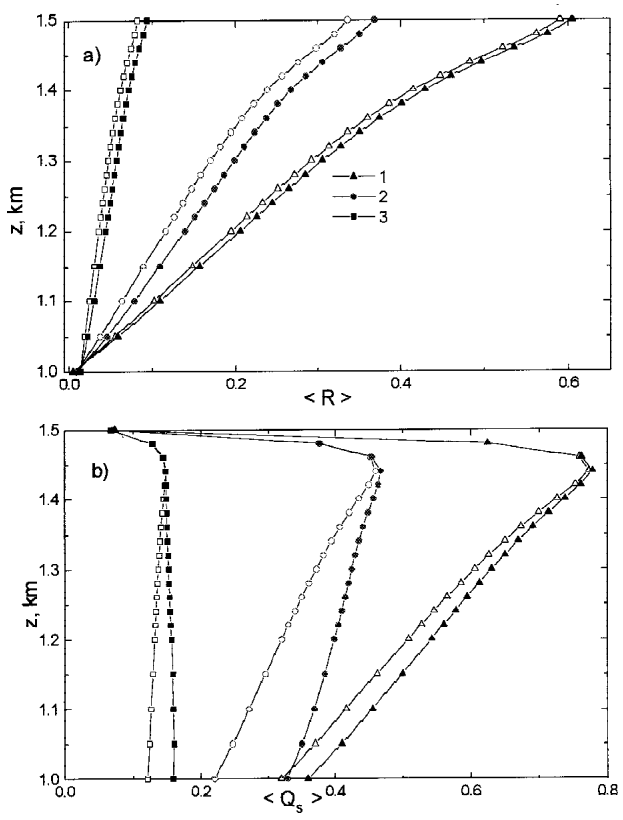

Figure 3. Dependence of the mean fluxes of upward (a) and downward (b) radiation on cloud fraction with $\sigma = 30\ km^{-1}$, $w_\lambda = 1$, $D = 1\ km$, $\xi_\oplus = 60°$, $A_s = 0$; $N = 0.1(1)$, $N = 0.5(2)$, $N = 0.9(3)$.

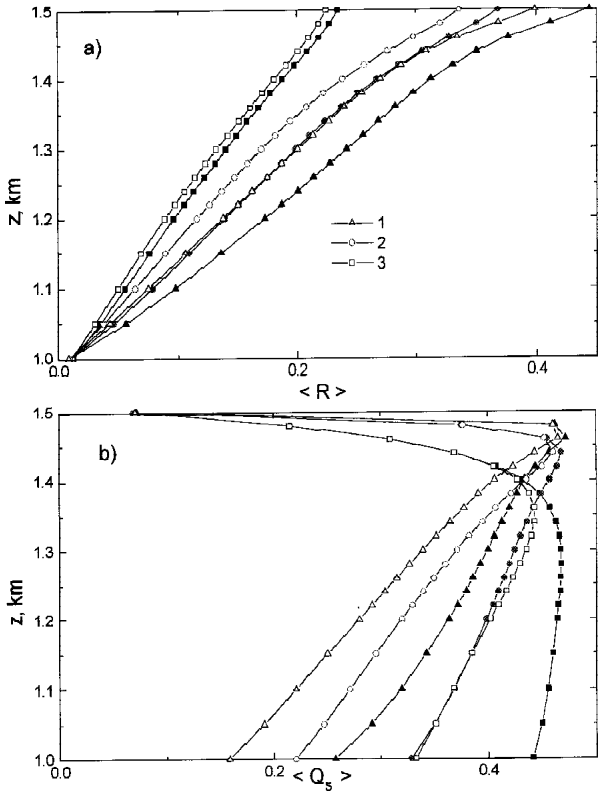

Figure 4. Vertical profiles of upward (a) and downward (b) fluxes with $w_\lambda = 1$, $N = 0.5$, $D = 1.0\ km$, $\xi_\oplus = 60°$, $A_s = 0$ and for different cloud extinction coefficients: $\sigma = 10(1)$, $30(2)$, $60(3)\ km^{-1}$.

$$P(z_1, z_{M+1}) = \sum_{i=1}^{M} P(z_i, z_{i+1}).$$

The relative absorption throughout a sublayer of thickness (z_i, z_{i+1}) is calculated as

$$p_j(z) = \frac{P(z_i, z_{i+1})}{(z_{i+1} - z_i)}$$

In computations, sublayers of variable thickness were used, namely 0.5-*km* thick layers between altitudes 1.0 and 1.2 *km*, and 0.02-*km* thick between 1.2 and 1.5 *km*.

Obviously, for a given single scattering albedo, the absorption will grow with an increase in the fraction of diffuse radiation and the mean scattering order. For stratus clouds, increasing the zenith solar angle reduces the absorption (Table 1); this results from the growth of the albedo of the cloudy layer and perhaps from a possible decrease in the mean scattering order of reflected radiation due to strong forward elongation of the scattering phase function. This result is consistent with findings by Davies et al. (1984).

For cumulus, the situation is quite the opposite because of a rapid growth of the fraction of diffuse radiation at large $\xi_\oplus$. For $\xi_\oplus = 0°$, the inequality $P_{St}(z_1, z_{M+1}) > P_{Cu}(z_1, z_{M+1})$ holds as a result of the fact that radiation exiting through the sides of cumulus clouds has, on the average, suffered fewer scattering interactions. At $\xi_\oplus = 60°$, the effect associated with the increase, on average, of the fraction of diffuse radiation dominates over that due to the decrease of the mean scattering order, so that the above inequality is reversed.

At $A_s = 0$, the histograms $p_j(z)$ have maxima located in the upper portion of the cloudy layer whose positions and magnitudes depend upon cloud type (Figure 5). The $p_j(z)$ and Q_s maxima are spatially correlated (cf. Figure 2), so this portion of the cloudy layer can be thought of as a region of most intensive scattering. For large surface albedo, the $p_j(z)$ increases most markedly in the lower and middle portions of the cloudy layer, thus reducing the vertical gradients of $p_j(z)$ compared with the $A_s = 0$ case. This is due to diffuse radiation, reflected from the surface and scattered in the under-cloud atmosphere, that illuminates the lower cloud boundary.

Table 1. The Mean Absorption in the Cloudy Layer, $P(z_1, z_{M+1})$, with $\sigma = 30\ km^{-1}$, D = 1 *km*, N = 0.5, and $A_s = 0$.

w_λ	$\xi_\oplus = 0°$		$\xi_\oplus = 60°$	
	St	*Cu*	*St*	*Cu*
0.99	0.125	0.105	0.116	0.127
0.9	0.420	0.399	0.393	0.494

With growing A_s, the histograms $p_{i,Cu}(z)$ increase faster than $p_{i,St}(z)$. This is attributable to the fact that the sides of numerous cumulus clouds act to reduce the mean flux of direct radiation of the above indicated diffuse source and, hence, to increase, on the average, the fraction of scattered radiation. We note that, for high A_s values, the histograms $p_{i,Cu}(z)$ may additionally have maxima in the lower portion of the cloudy layer.

Let us discuss briefly the influence of the atmospheric gaseous absorption on the mean spectral fluxes of the near-IR solar radiation. Figure 6 illustrates profiles of the upward and downward radiation for wavelength $\lambda = 1.43$ μm at which the absorption due to water vapor and carbon dioxide takes place. The gaseous absorption produces an appreciable depletion of the upward and downward fluxes in the above-cloud atmosphere. Most strong atmospheric gaseous absorption occurs in the cloudy layer in which the gases are assumed to be in sufficient concentrations and the photon paths, due to multiple scattering, are substantially lengthened.

Conclusions

At $A_s = 0$, upward fluxes may differ by as much as ≈20% when computed at the upper boundaries of cumulus and stratus clouds. Within the cloudy layer, downward fluxes of diffuse solar radiation, as functions of altitude, may have maxima whose magnitudes and locations depend upon optic and geometric parameters of the cloud field and upon the solar zenith angle. At $\xi_\oplus = 60°$, the downward flux of diffuse radiation at a lower cloud boundary is nearly two times larger for cumulus than for stratus.

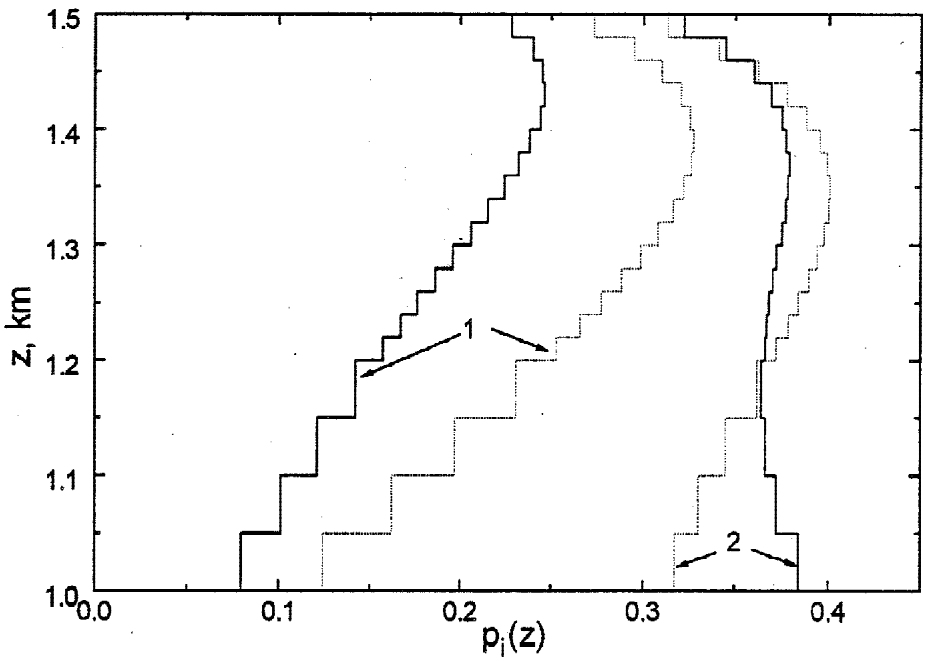

Figure 5. Vertical profiles of absorption $p_i(z)$ with $\sigma = 30\ km^{-1}$, $w_\lambda = 0.99$, $N = 0.5$, $D = 0.25\ km$, $\xi_\oplus = 0°$ and for different surface albedos and cloud types: $A_S = 0(1), 0.8(2)$, cumulus (solid lines), and stratus (dot lines).

For $A_S > 0$, radiation reflected from the surface and scattered in the under-cloud atmosphere plays a role of a diffuse source illuminating the cloud lower boundary and modifying boundary conditions. This is why the vertical profiles of radiative fluxes differ qualitatively from those in the $A_S = 0$ case.

Aerosol particles present in the cloud layer as condensation nuclei produce absorption that is essentially cloud-type dependent. In particular, as the solar zenith angle increases from $\xi_\oplus = 0°$ to $\xi_\oplus = 60°$, the absorption decreases in stratus, increases in cumulus. Further, the albedo of the underlying surface is an important parameter governing the distribution of absorption over the cloudy layer. While for the $A_S = 0$ case the absorption is maximum in the upper portion of cloud layer, when A_S is large, a maximum absorption may occur in the vicinity of the cloud lower boundary.

Acknowledgment

This work was partially supported by the U.S. Department of Energy's Atmospheric Radiation Measurement Program.

References

Davies, R., W. L. Ridgway, and K.-E. Kim. 1984. Spectral absorption of solar radiation in cloudy atmospheres: A 20 cm^{-1} model. *J. Atmos. Sci.* **41**:2126-2137.

Ellingson, R. G., J. Ellis, and S. Fels. 1991. Intercomparing of radiation codes used in climate models: Long wave results. *J. Geophys. Res.* **96**(D5):8929-8954.

Filippov, V. A. 1973. Some results of numerical experiment to substantiate the choice of the parameters of the

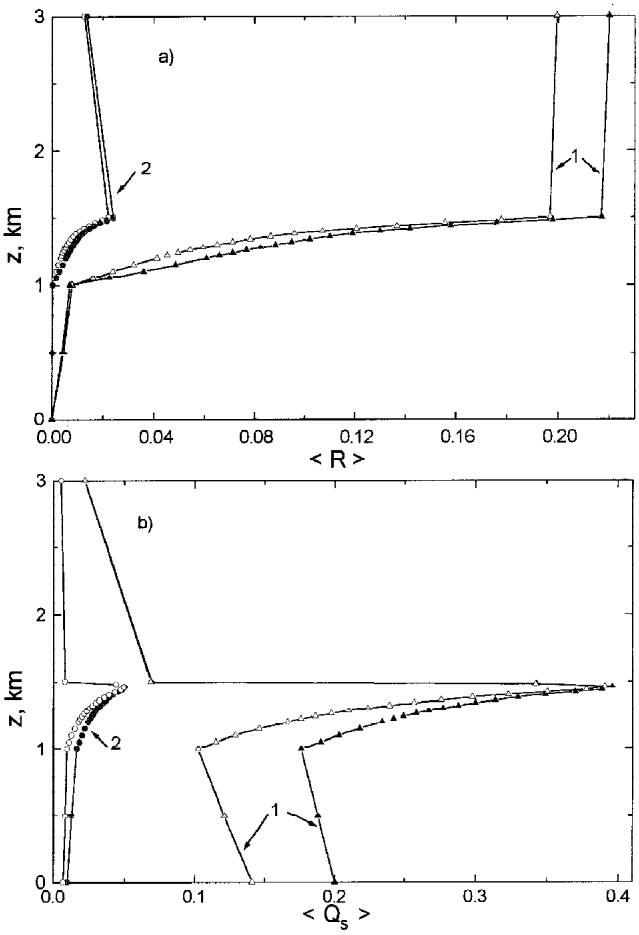

Figure 6. Upward (a) and downward (b) radiative fluxes at wavelength λ = 1.43 μm with σ = 30.89 km^{-1}, w_λ = 0.967, N = 0.5, D = 1 km, $\xi_\oplus$ = 60°, and A_s = 0. Computations without (1) and with (2) accounting for the absorption due to water vapor and carbon dioxide.

transmission functions of atmospheric gases with unresolved structure of spectrum. *Izv. Acad. Sci. USSR Atmos. Oceanic Phys.* **9**:774-775.

Fouquart, Y., B. Bonnel, and V. Ramaswamy. 1991. Intercomparing shortwave radiation codes for climate studies. *J. Geophys. Res.* **96**(D5):8955-8968.

Golubitskii, B. M., and N. I. Moskalenko. 1968. Spectral transmission functions in the H_2O vapor and CO_2 bands. *Izv. Acad. Sci. USSR Atmos. Oceanic Phys.* **4**: 346-359.

Moskalenko, N. I. 1969. Spectral transmission functions in the bands of H_2O vapor and O_3, N_2O, and N_2 constituents of the atmosphere. *Izv. Acad. Sci. USSR Atmos. Oceanic Phys.* **5**:1179-1190.

Skorinov, V. N., and G. A. Titov. 1984. On accuracy of an approximation method for calculating radiant fluxes in broken cloudiness. *Izv. Acad. Sci. USSR Atmos. Oceanic Phys.* **20**:263-270.

Titov, G. A. 1987. Sensitivity of the mean radiant fluxes to the variations in the parameters of broken clouds. *Izv. Acad. Sci. USSR Atmos. Oceanic Phys.* **23**:851-858.

Titov, G. A. 1989. *Statistical description of the optical radiative transfer in clouds*. Doct. Phys.-Math. Sci. Dissert. Institute of Atmospheric Optics, Tomsk.

Zhuravleva, T. B. 1993. *Statistical characteristics of solar radiation in broken Clouds*. Cand. Phys.-Math. Sci. Dissert. (05.13.16). Institute of Atmospheric Optics, Tomsk.

Zuev, V. E., and V. S. Komarov. 1986. *Statistical Models of Temperature and Gas Constituents in the Atmosphere.* Leningrad, Gidrometeoizdat.

Zuev, V. E., and G. M. Krekov. 1986. *Optical Models of Atmosphere*. Leningrad, Gidrometeoizdat.

Zuev, V. E., and G. A. Titov. 1994. Radiative Transfer in Clouds Fields with Random Geometry *J. Atmos. Sci*. **52**:176-190.